Synthesis and Characterization of Tetrapodal Nickel Complexes with Adaptable Ligand Binding Geometries.

Hsien-Liang Cho,[a] Kelly L. Gullet,[b] and Alison R. Fout[a*]

[a] Department of Chemistry, Texas A&M University, College Station, TX 77843, USA
[b] School of Chemical Sciences, University of Illinois at Urbana-Champaign, 600 S. Mathews Ave. Urbana, IL 61801, USA

Table of Contents

General considerations:

Materials and Methods.

All manipulations were carried out in the absence of water and dioxygen, due to the air and moisture sensitivity of the compounds, using a Vigor inert atmosphere glovebox under a nitrogen atmosphere unless otherwise specified. All glassware was dried in an oven for at least 4 h and cooled in an evacuated antechamber prior to use. Solvent was dried and deoxygenated on a Vigor Solvent Purification System and stored over 4 Å molecular sieves (3 Å for MeCN), purchased from VWR, prior to use. Deuterated solvents were purchased from Cambridge Isotope Laboratories and stored over 3 Å molecular sieves prior to use. Celite 545 (J. T. Baker) was heated to 150 °C under dynamic vacuum for 24 h prior to use in the drybox. All reagents were purchased from commercial sources and used as received unless otherwise noted. 2,6-lutidinium triflate (LuOTf)[1] and $Py_2Py(pi^{Cy})_2$were synthesized according to literature procedures.[2]

Physical methods.

^{1}H NMR spectra were recorded at ambient temperature on a Bruker Avance Neo console operating at 400 MHz (^{1}H NMR) and 126 (^{13}C NMR). Solid-state infrared spectra were measured using a Perkin Elmer Frontier FT-IR spectrophotometer equipped with a KRS5 thallium bromide/iodide universal attenuated total reflectance accessory. Single crystal x-ray diffraction studies were conducted on Venture Bruker-AXS CPAS IuS copper source kappa, Quest Bruker AXS CPAD IuS molybdenum source three-circle, or Rigaku XtaLAB Synergy, Dualflex, HyPix 6000He X-ray diffractometers at the Texas A&M X-Ray Diffraction Laboratory. Single crystal X-ray diffraction measurements were carried out at a low temperature employing a (three circle or kappa) Bruker-AXS (Quest or Venture) with IμS source and a Photon III area detector diffractometer for (Mo Kα radiation, λ = 0.71073 Å or Cu Kα radiation, λ = 1.54178 Å) (NSF-CHE-9807975, NSF-CHE-0079822 and NSF-CHE-0215838) and cooled in a cold nitrogen stream (OXFORD Crysosystems (700 or 800)), to 110(2) K. Bruker AXS APEX 3[3] software was used for data collection and reduction. Absorption corrections were applied using SADABS.[4] Space group assignments were determined by examination of systematic absences, E-statistics, and successive refinement of the structures. Structures were solved using SHELXT[5] and refined by least-squares refinement on F^2 followed by difference Fourier synthesis (OLEX2, SHELXL).[6, 7] Data were collected using a XtaLAB Synergy, Dualflex, HyPix 6000He diffractometer equipped with an Oxford Cryosystems low-temperature device operating at 100 K. The diffraction pattern was indexed and the total number of runs and images was based on the strategy calculation from the program CrysAlisPro 1.171.42.101a (Rigaku OD, 2023).[8] Data reduction, scaling and multi-scan absorption corrections were performed using CrysAlisPro 1.171.42.101a (Rigaku OD, 2023). Empirical absorption correction using spherical harmonics, implemented in SCALE3 ABSPAC scaling algorithm. Ultraviolet-visible (UV-vis) spectroscopy was performed on an Agilent Technologies Cary Series UV-vis NIR 5000 spectrometer. All samples were prepared in a drybox containing a dinitrogen atmosphere in quartz cuvettes with a 1 cm path length and capped with a rubber septum. Magnetic data were collected on a Quantum Design SQUID-VSM magnetometer at 1 T from 2-300 K. SQUID measurements were done at MSEN Department, Texas A&M University.

Experimental Procedures:

Synthesis of Metal Compounds

Synthesis of $Py_3(pi^{Cy})_2Ni$ (**1**)

A 20 mL scintillation vial was charged with $Py_2Py(pi^{Cy})_2$ (0.097 g, 0.152 mmol) and 2 mL of tetrahydrofuran (THF). KH (0.013 g, 0.319 mmol) was added to the pale brown solution, forming a pink solution. After stirring for 30 minutes, excess KH was removed via filtration over a pad of celite and then $NiOTf_2$ (0.054 g, 0.152 mmol) was added to the filtrate. The solution changed color from pink to an orange-red over the course of the reaction. The reaction proceeded for 24 h followed by removal of volatiles under reduced pressure. The orange-red solid precipitate was washed with diethyl ether (2 mL) and collected by elution of benzene (6 mL) (0.090 g, 0.130 mmol, 85%). Crystals suitable for single crystal X-ray analysis were grown from layer diffusion of pentane and diethyl ether (ratio??) into a concentrated solution of dichloromethane at room temperature. ^{1}H NMR (400 MHz, 298 K, C_6D_6) δ 8.53 (d, J = 4.5 Hz, 2H), 7.23 (d, J = 8.0 Hz, 2H), 7.13 (d, J = 9.0 Hz, 2H), 6.94 (s, 2H), 6.91 – 6.81 (m, 5H), 6.78 (d, J = 3.8 Hz, 2H), 6.64 (dd, J = 7.2, 4.7 Hz, 2H), 6.24 (d, J = 3.9 Hz, 2H), 2.77 (s, 3H), 2.69 (t, J = 11.1 Hz, 2H), 2.20 (s, 3H), 1.82 (d, J = 12.2 Hz, 2H), 1.75 (d, J = 12.8 Hz, 2H), 1.58 (d, J = 13.1 Hz, 4H), 1.45 (d, J = 13.3 Hz, 2H), 1.16 – 1.02 (m, 4H), 1.00 – 0.80 (m, 7H). ^{13}C NMR (126 MHz, 298 K, C_6D_6) δ 167.41, 164.89, 164.63, 156.35, 152.63, 148.70, 137.99, 136.20, 135.13, 124.53, 120.88, 120.37, 119.78, 117.50, 110.20, 61.18, 59.88, 50.66, 34.71, 34.57, 28.54, 27.56, 26.49, 26.45, 25.89. IR: ν = 1573 cm^{-1} (C=N). ESI–HRMS: calculated $[C_{41}H_{46}N_7Ni]^+$: 694.3163, found: 694.3153.

Synthesis of $[Py_2Py(afa^{Cy})_2Ni]OTf_2$ (**2**)

To a 20 mL scintillation vial were added $Py_3(pi^{Cy})_2Ni$ (0.019 g, 0.027 mmol), 3 mL of acetonitrile and benzene mixture (2:1), and 2,6-lutidinium triflate (0.014 g, 0.054 mmol). The solution was stirred for 16 h, changing from an orange to a light brown solution, and then dried in *vacuo*. The brown solid was washed with diethyl ether (2 mL) to remove 2,6-dimethylpyrdine and eluted with acetonitrile (8 mL) to isolate $[Py_2Py(afa^{Cy})_2Ni]OTf_2$. Volatiles were removed under reduced pressure to give a light-brown powder (0.025mg, 0.025 mmol, 93%). Crystals suitable for single crystal X-ray analysis were grown from vapor diffusion of diethyl ether into a concentrated solution of acetonitrile at room temperature. ^{1}H NMR (400 MHz, 298 K, CD_3CN) δ 66.95, 50.89, 44.62, 41.51, 37.29, 17.78, 16.96, 9.24, 7.28, 7.22, 7.17, 6.73, 6.10, 5.47, 2.50, 1.15. μ_{eff} (SQUID) = 2.88 μ_B (300 K). IR: ν = 1631 (C=N), 3209, 3282 cm^{-1}. ESI–HRMS: calculated $[C_{41}H_{47}N_7Ni]^{2+}$: 347.6618, found: 347.6611.

Synthesis of $[Py_2Py(afa^{Cy})_2Ni(OH)]OTf$ (**3**-OTf)

To a 20 mL scintillation vial were added $[Py_2Py(afa^{Cy})_2Ni]OTf_2$ (0.018 g, 0.018 mmol), KOH (0.002 g, 0.036 mmol), and 2 mL of acetonitrile. The reaction was stirred for 2 h, and a yellow-white precipitate started to form overtime. The volatiles were then removed under reduced pressure. The resulting precipitate was dissolved in dichloromethane (4 mL) and filtered over a pad of celite. The dichloromethane filtrate was dried in *vacuo*, forming a pale-yellow powder (0.015 g, 0.017

mmol, 97%). ^{1}H NMR (400 MHz, 298 K, CD_3CN) δ 64.87, 50.42, 49.02, 39.81, 37.41, 36.72, 15.67, 8.47, 6.66, 4.17, 2.54, 1.72. ^{19}F NMR (377 MHz, 298 K, CD_3CN) δ -79.31. μ_{eff} (SQUID) = 3.38 μ_B (300 K). IR: ν = 1663 cm^{-1} (C=N). ESI–HRMS: calculated $[C_{41}H_{48}N_7NiO]^+$: 712.3268, found: 712.3257.

Synthesis of $[Py_2Py(afa^{Cy})_2Ni(OH)]PF_6$ (**3**-PF_6)

To a 20 mL scintillation vial were added $[Py_2Py(afa^{Cy})_2Ni(OH)]OTf$ (0.021 g, 0.026 mmol), and 3 mL of THF. After dissolution, $NaPF_6$ (0.004 g, 0.026 mmol) was added to the solution. After stirring for 1 h at room temperature, volatiles were removed *in vacuo*. The resulting precipitate was dissolved in dichloromethane (4 mL) and filtered over a pad of celite. The volatiles were then removed under reduced pressure, producing a pale-yellow powder (0.017 mg, 0.019 mmol, 77%). Crystals suitable for single crystal X-ray analysis were grown from layer diffusion of diethyl ether into a concentrated solution of dichloromethane and THF (2:1) at room temperature. ^{1}H NMR (400 MHz, CD_3CN) δ 64.86, 50.41, 49.03, 39.81, 37.41, 36.75, 15.66, 8.50, 7.62, 7.42, 7.18, 7.09, 7.08, 6.87, 6.52, 6.17, 5.73, 5.47, 5.26, 5.16, 4.06, 3.74, 3.66, 2.33, 2.27, 2.22, 2.01, 1.87, 1.82, 1.73. ^{19}F NMR (377 MHz, 298 K, CD_3CN) δ -72.79 (d, J = 706.6 Hz).

Synthesis of $Py_2Py(pi^{Cy})_2NiOH_2$ (**4**)

Outside the glovebox, to a 20 mL scintillation vial were added $Py_2Py(pi^{Cy})_2$ (0.022 g, 0.035 mmol), $Ni(OAc)_2{\cdot}4H_2O$ (0.087 g, 0.035 mmol), and 2 mL of methanol. After stirring at room temperature for 16 h, the volatiles were removed under reduced pressure. The brown-red residue was dissolved in dichloromethane (6 mL) and filtered over a pad of celite. The volatiles were again removed under reduced pressure, yielding a brown-red powder which was assigned $[Py_2Py(afa^{Cy})_2Ni(OH)]OAc$ (0.026 g, 0.033 mmol, 96%) based on ^{1}H NMR and IR spectroscopy. Crystals suitable for single crystal X-ray analysis were grown from layer diffusion of hexane and diethyl ether (10:1) into a concentrated solution of dichloromethane at room temperature, forming an aqua complex. The poor solubility of the complex precluded its characterization by ^{1}H NMR spectroscopy. μ_{eff} (SQUID) = 1.77 μ_B (300 K). IR: ν = 1620 cm^{-1} (C=N).

Synthesis of $[Py_3(pi^{Cy})_2Ni(Ag)]OTf$ (**5**)

To a 20 mL scintillation vial was added $Py_3(pi^{Cy})_2Ni$ (0.020 g, 0.028 mmol), and 2 mL of THF. The vial was wrapped in electrical tape to exclude light. AgOTf (0.007 g, 0.0028 mmol) was added to the orange solution; an immediate color change to red was observed. After stirring for 1 h, the red solution was filtered over a pad of celite and volatiles were removed under reduced pressure, yielding a red powder (0.026 g, 0.027 mmol, 96%). Crystals suitable for single crystal X-ray analysis were grown from layer diffusion of diethyl ether into a concentrated solution of acetonitrile at room temperature. ^{1}H NMR (400 MHz, 298 K, CD_3CN) δ 8.20 (d, J = 4.7 Hz, 2H), 7.81 – 7.70 (m, 3H), 7.47 – 7.38 (m, 6H), 7.35 – 7.26 (m, 4H), 6.53 (d, J = 4.4 Hz, 2H), 5.53 (d, J = 3.8 Hz, 2H), 2.87 (t, J = 10.4 Hz, 2H), 2.17 (s, 3H), 2.09 (d, J = 11.1 Hz, 3H), 2.03 (d, J = 10.9 Hz, 2H), 1.96 (s, 1H), 1.93 – 1.86 (m, 5H), 1.78 – 1.69 (m, 6H), 1.41 (dt, J = 23.5, 12.4 Hz, 9H), 1.30 – 1.15 (m, 2H). ^{13}C NMR (126 MHz, 298 K, CD_3CN) δ 165.28, 164.22, 163.02, 158.76, 151.34, 150.68, 139.27, 138.80, 123.99, 123.27, 121.49, 120.00, 117.76, 108.81, 61.16, 59.88,

50.85, 35.23, 35.18, 29.66, 28.00, 26.87, 26.27.IR: ν = 1573, 1634 cm^{-1} (C=N). ESI–HRMS: calculated $[C_{41}H_{45}N_7NiAg]^+$: 800.2135, found: 800.2122.

Alternative synthesis of **2** from **3**

To a 20 mL scintillation vial were added **3** (0.030 g, 0.035 mmol), 2 mL of acetonitrile, 2,6-lutidinium triflate (0.008 g, 0.031 mmol), and $MgSO_4$ (~20mg). The solution was stirred for 1 h, then volatiles were removed under reduced pressure. The light-brown solid was washed with diethyl ether (2 mL) to remove 2,6-dimethylpyrdine, and subsequently eluted with acetonitrile (8 mL). The volatiles were removed under reduced pressure to yield beige powder, **2** (0.032 g, 0.0032 mmol, 93%), confirmed by ^{1}H NMR spectroscopy.

Alternative synthesis of **1** from **2**

To a 20 mL scintillation vial were added **2** (0.022 g, 0.022 mmol), and 2 mL of THF. KH (0.002 g, 0.047 mmol) was then added to the brown suspension. A color change to orange was observed over the course of 30 minutes. Volatiles were removed under reduced pressure and the orange solid was eluted with benzene (6 mL). The product was confirmed as **1** (0.015 g, 0.022 mmol, 97%) by ^{1}H NMR spectroscopy.

Alternative synthesis of **4** from **2**

To a 20 mL scintillation vial were added **2** (0.032 g, 0.032 mmol), and 2 mL of acetonitrile. Li_2O (0.002 g, 0.063 mmol) was added to the brown suspension. The reaction was stirred for 16 h. Formation of a precipitate, **4**, was noted over the course of the reaction. The reaction was then filtered over a filter paper, and the beige powder, 4, was collected and dried in *vacuo*.

NMR spectra of Metal Complexes

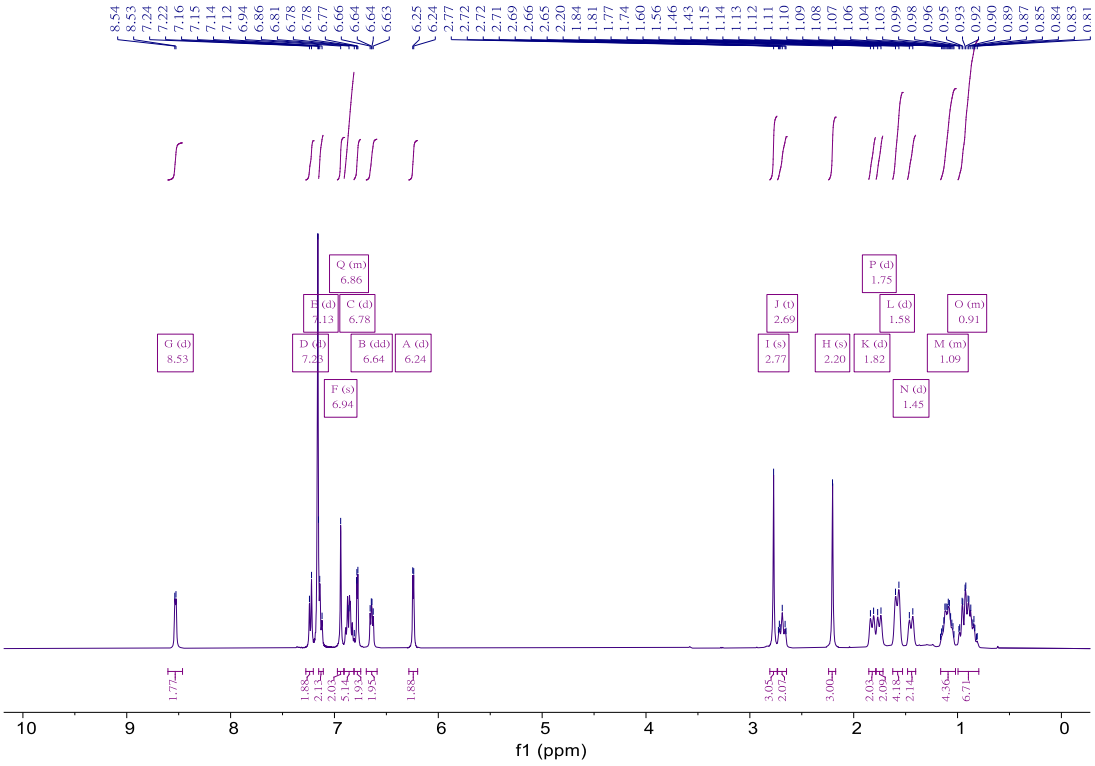

Figure S1. ^{1}H NMR (400 MHz, C_6D_6, 298 K) spectrum of $Py_3(pi^{Cy})_2Ni$.

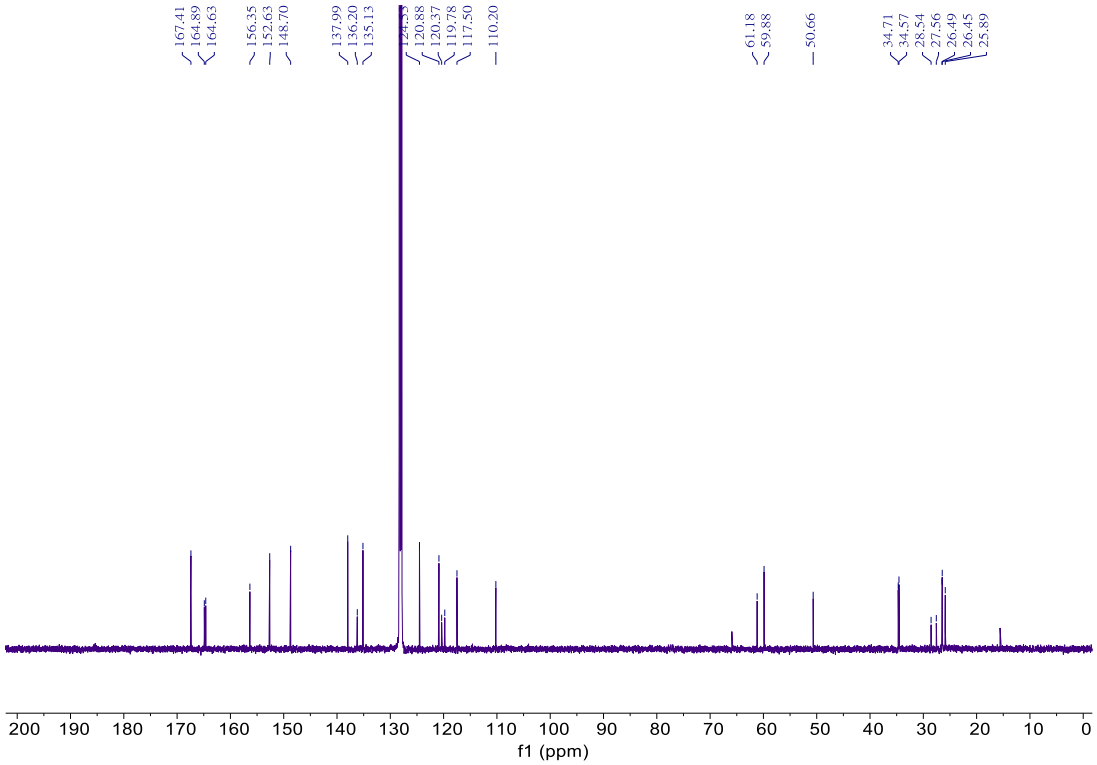

Figure S2. ^{13}C NMR (126 MHz, C_6D_6, 298 K) of $Py_3(pi^{Cy})_2Ni$.

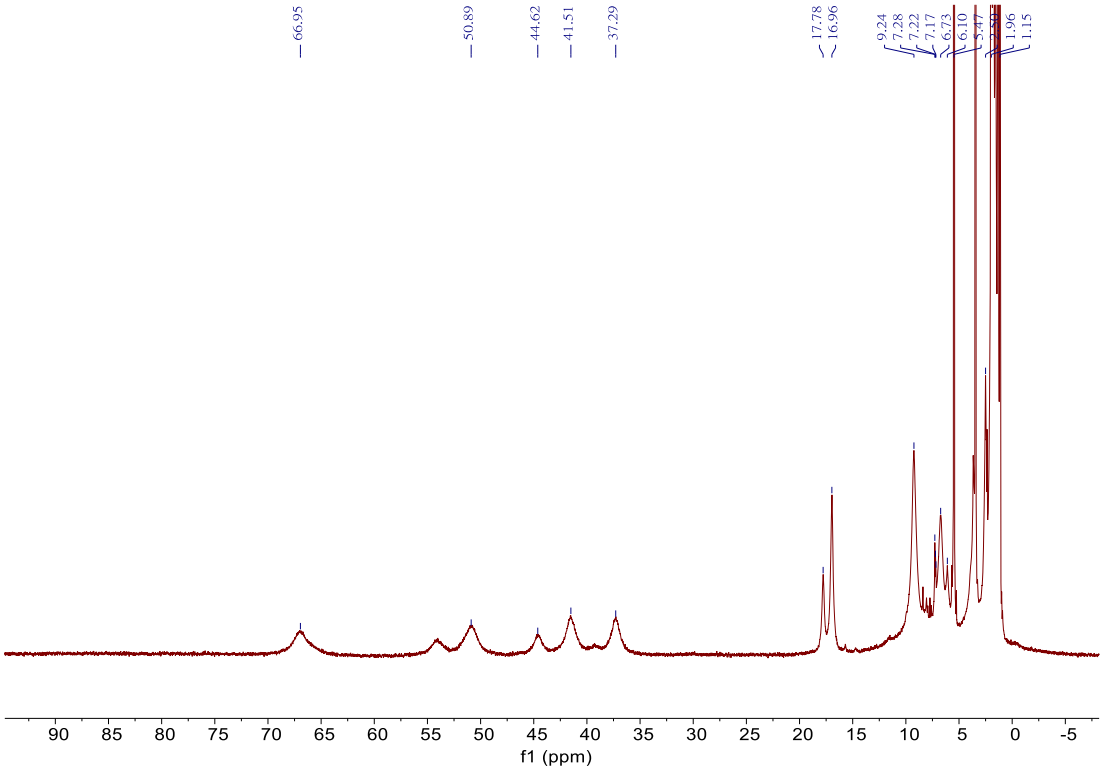

Figure S3. ^{1}H NMR (400 MHz, CD_3CN, 298 K) of $[Py_2Py(afa^{Cy})_2Ni]OTf_2$.

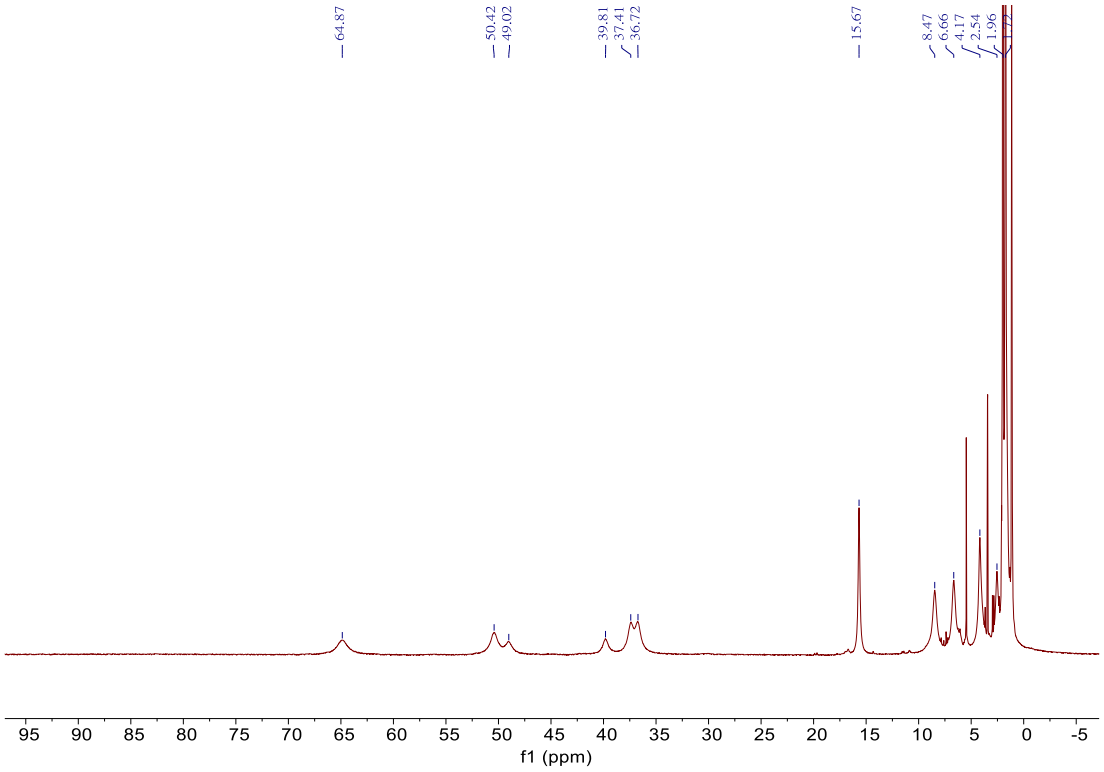

Figure S4. ^{1}H NMR (400 MHz, CD_3CN, 298 K) of $[Py_2Py(afa^{Cy})_2Ni(OH)]OTf$.

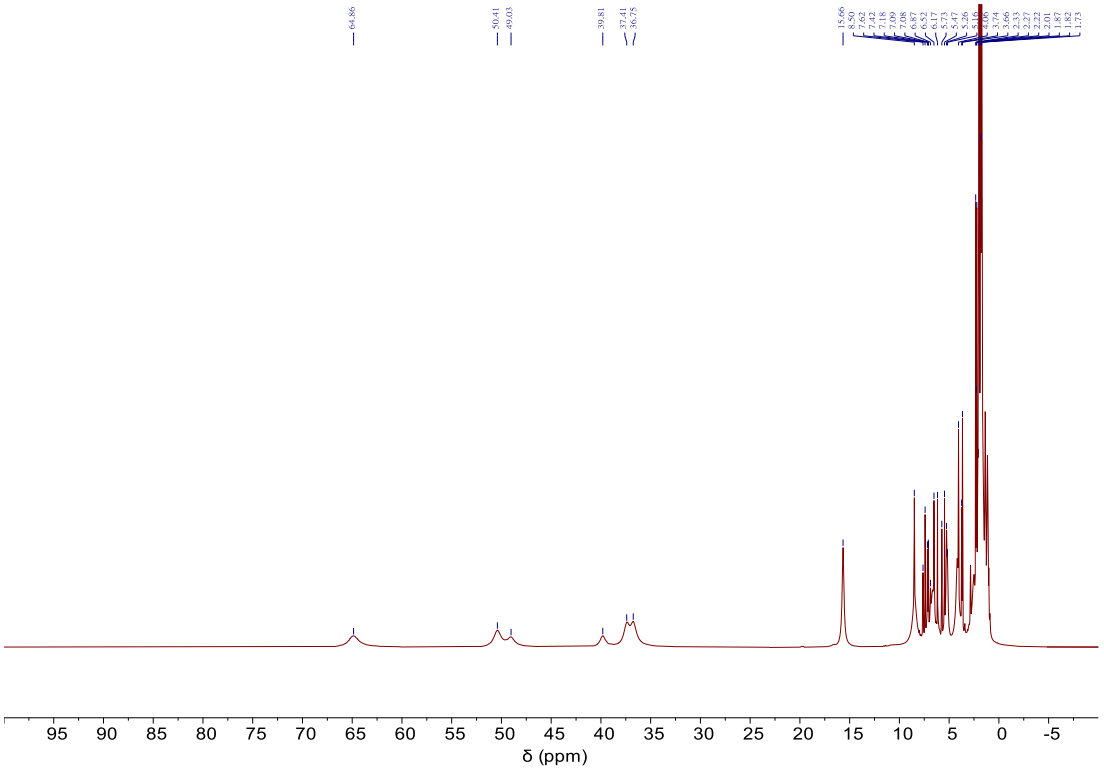

Figure S5. ^{1}H NMR (400 MHz, CD_3CN, 298 K) of $[Py_2Py(afa^{Cy})_2Ni(OH)]PF_6$.

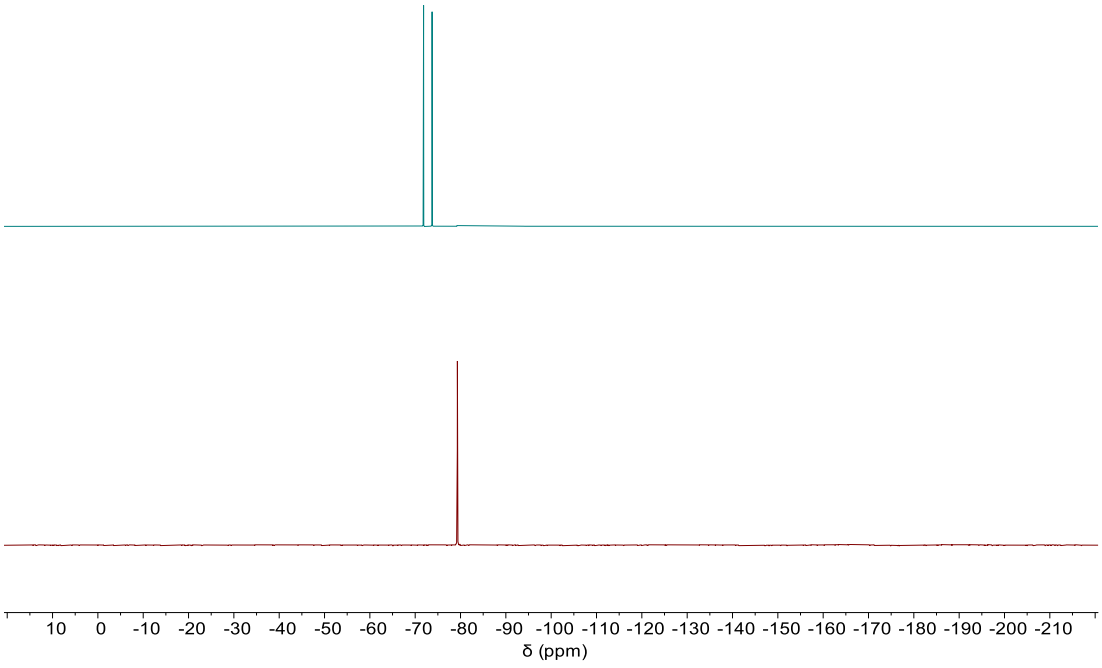

Figure S6. ^{19}F NMR (377 MHz, CD_3CN, 298 K) of $[Py_2Py(afa^{Cy})_2Ni(OH)]PF_6$ (top) and $[Py_2Py(afa^{Cy})_2Ni(OH)]OTf$ (bottom).

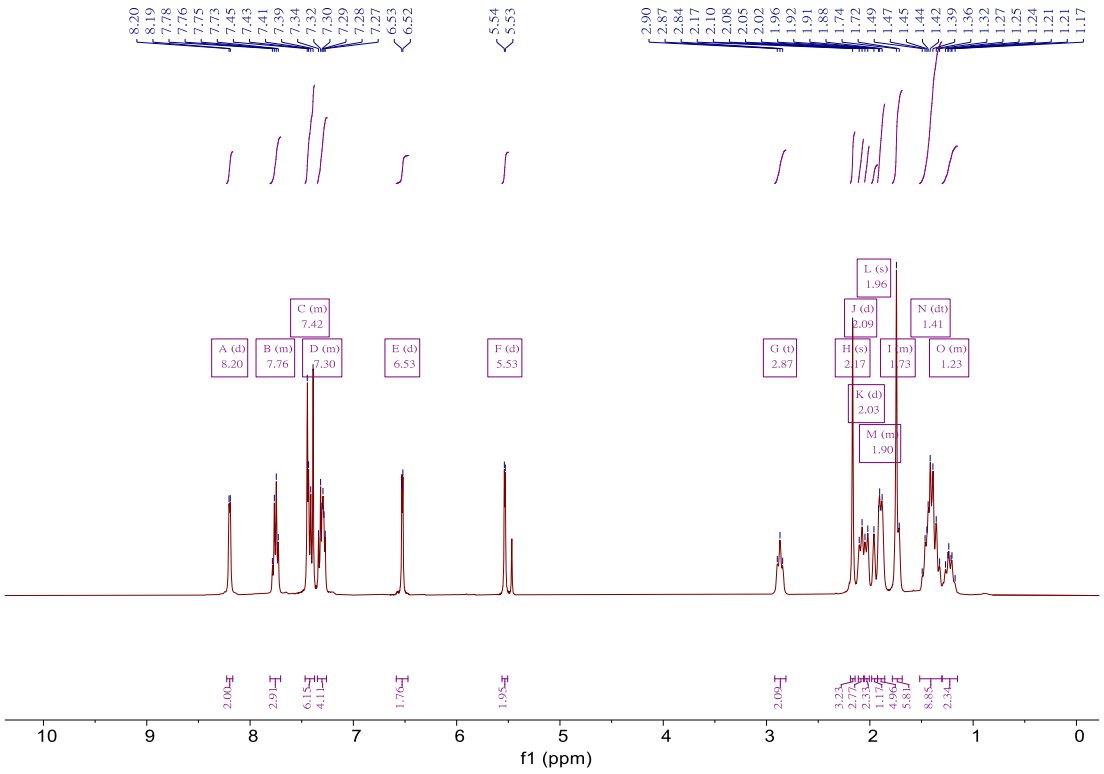

Figure S7. ^{1}H NMR (400 MHz, CD_3CN, 298 K) of $[Py_3(pi^{Cy})_2Ni(Ag)]OTf$.

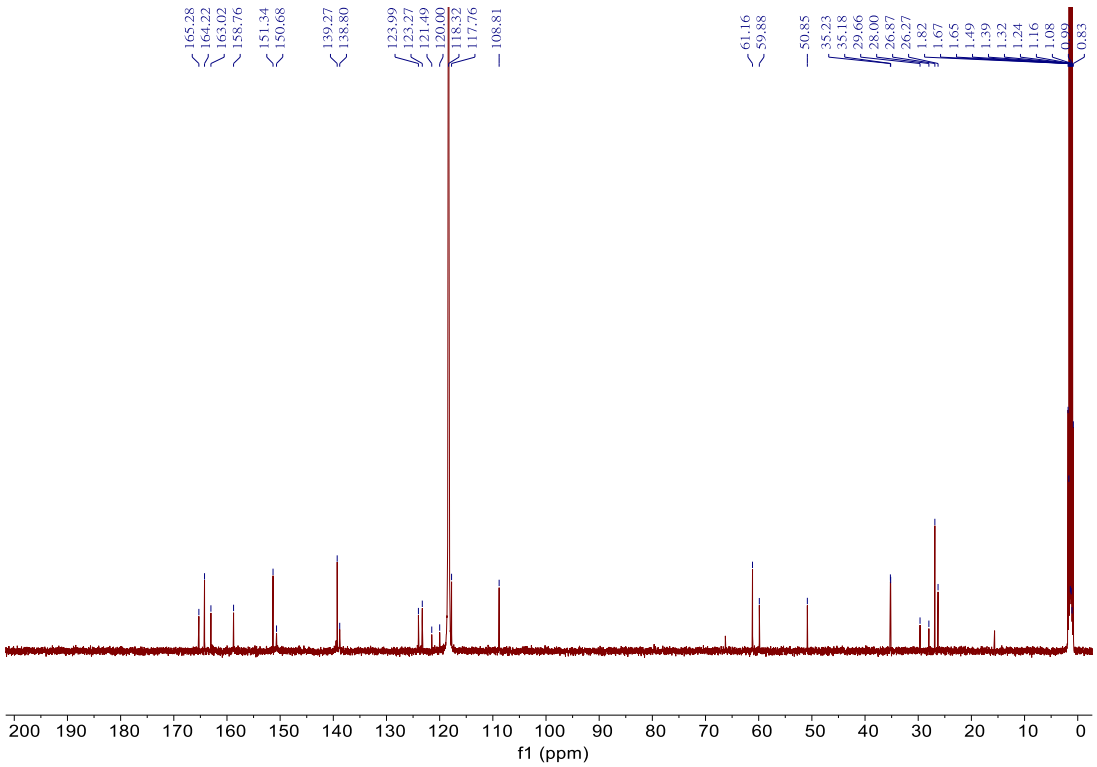

Figure S8. ^{13}C NMR(126 MHz, CD_3CN, 298 K) of $[Py_3(pi^{Cy})_2Ni(Ag)]OTf$.

FT-IR spectra of Metal Complexes

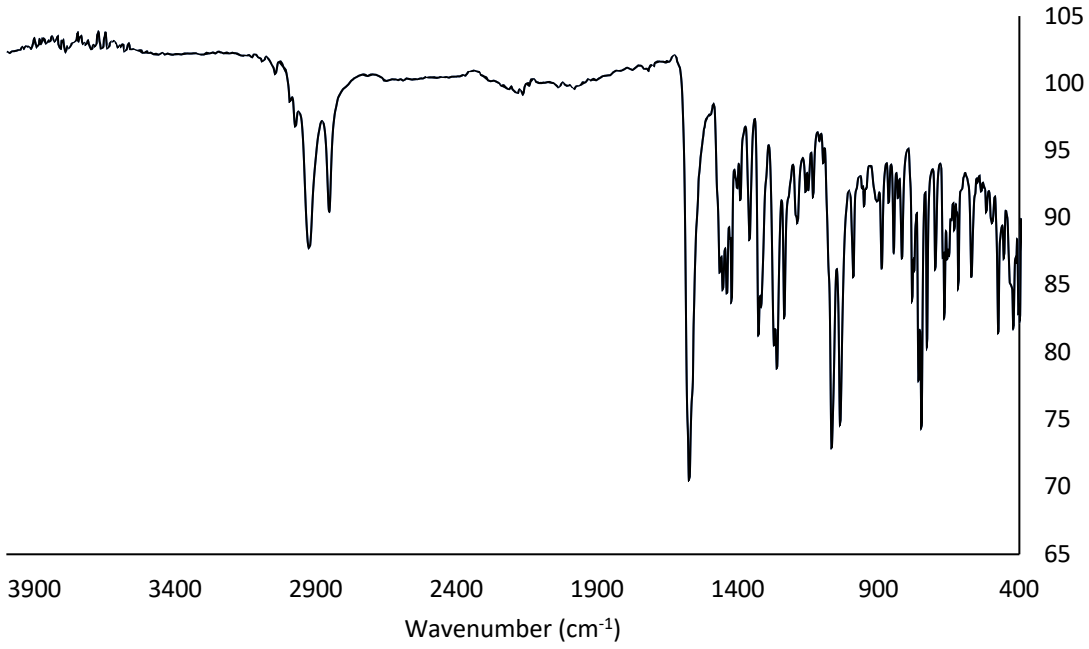

Figure S9. FT-IR spectrum of $Py_3(pi^{Cy})_2Ni$.

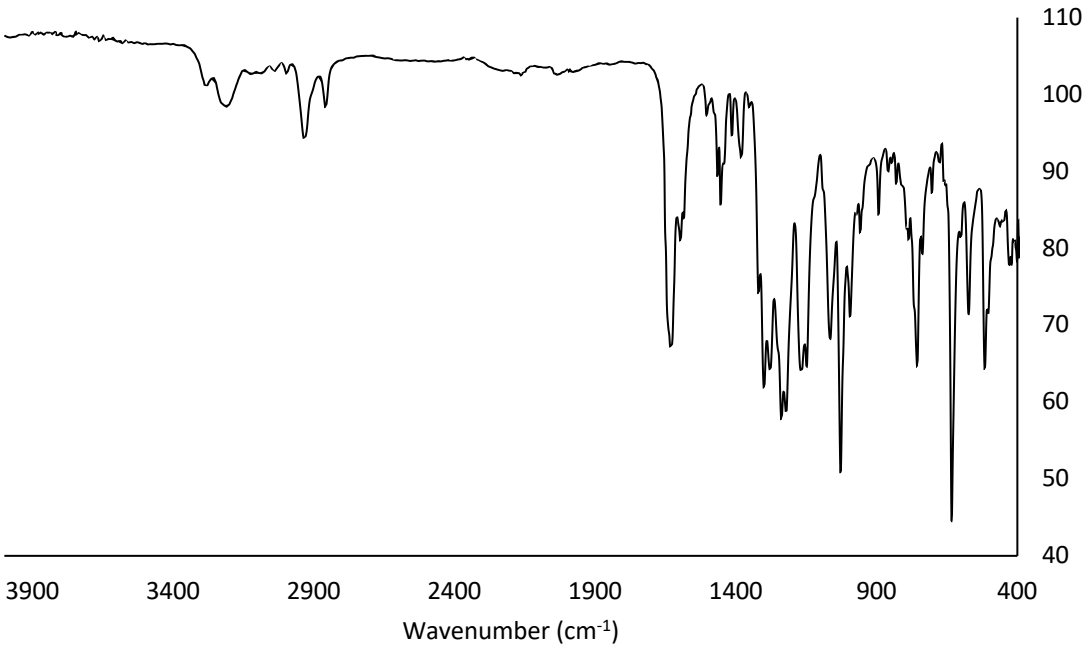

Figure S10. FT-IR spectrum of $[Py_2Py(afa^{Cy})_2Ni]OTf_2$.

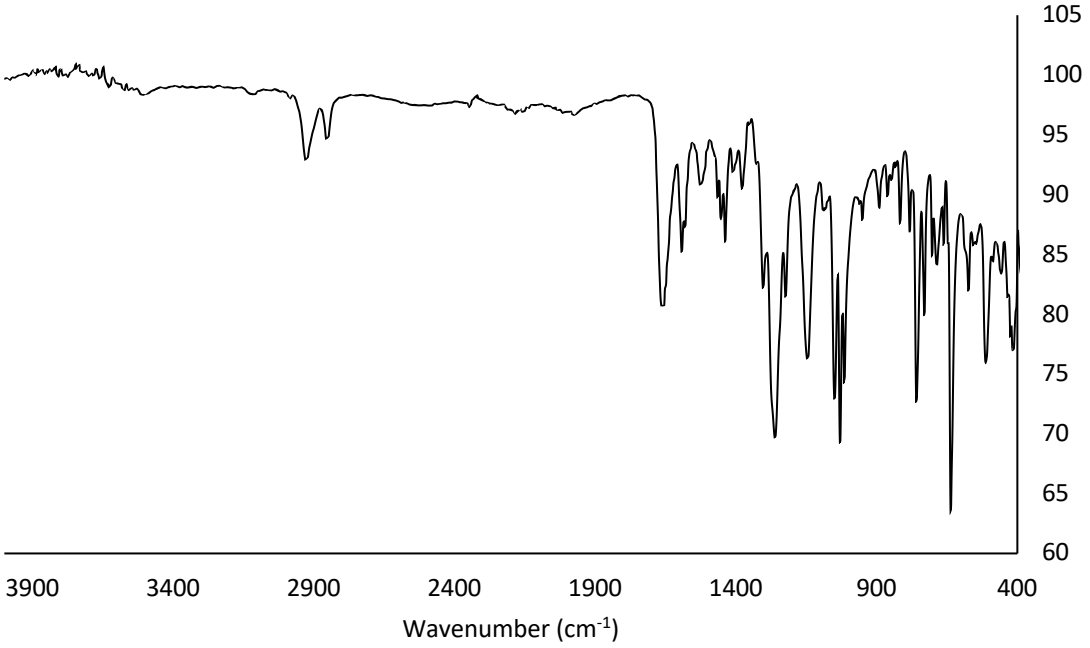

Figure S11. FT-IR spectrum of $[Py_2Py(afa^{Cy})_2Ni(OH)]OTf$.

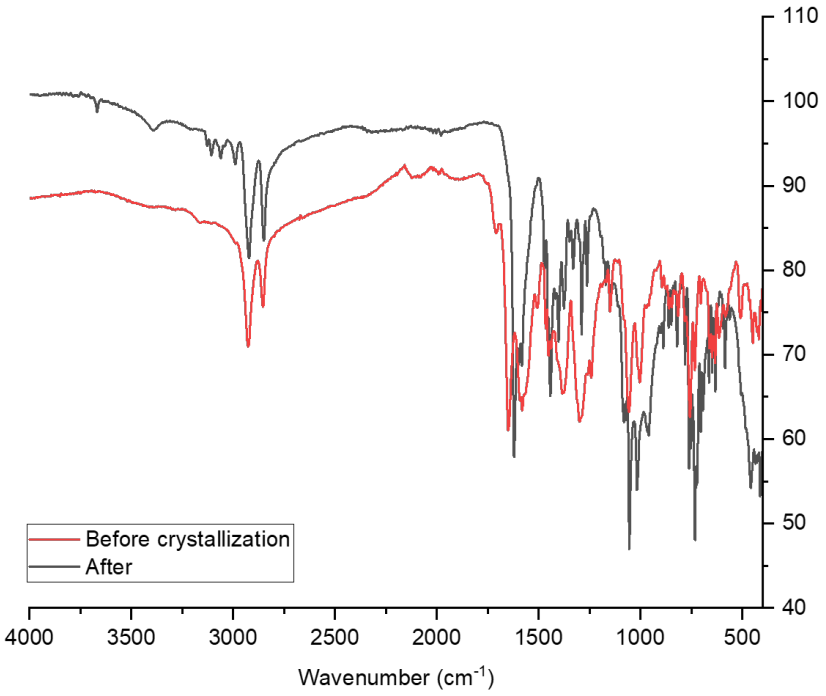

Figure S12. FT-IR spectrum of $Py_2Py(Pi^{Cy})_2$ + $NiOAc_2 \cdot 4H_2O$ reaction.

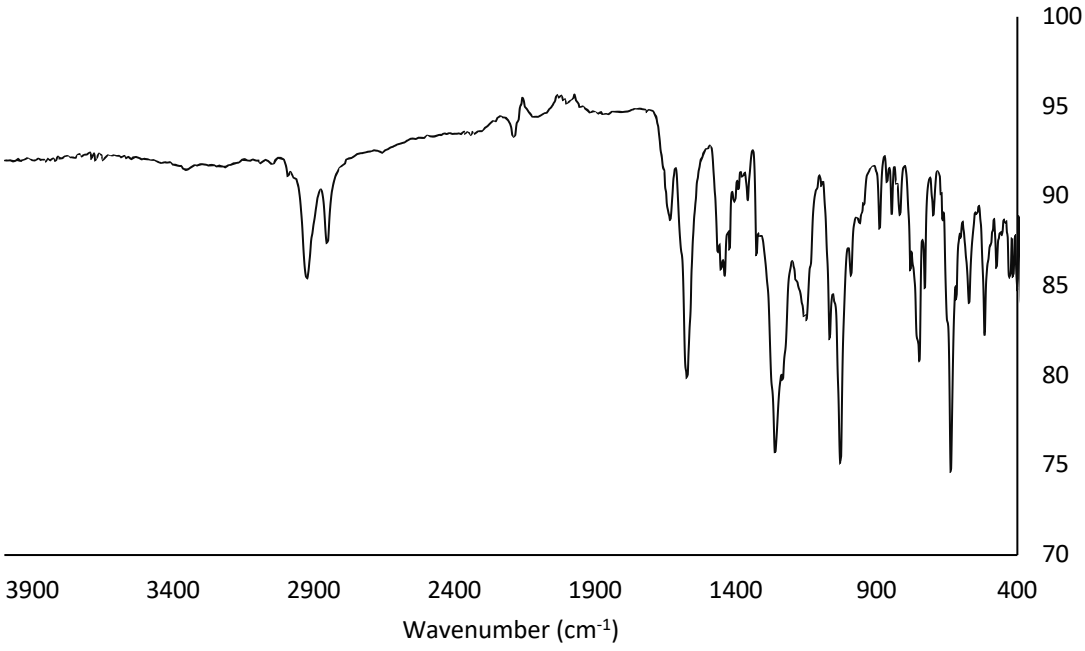

Figure S13. FT-IR spectrum of $[Py_3(pi^{Cy})_2Ni(Ag)]OTf$.

General Conditions for initial rate studies.

Various equivalents of lutidinium trifalte and temperatures:

1 was weighted into a 2 mL volumetric flask and diluted to 2 mL to form a MeCN/benzene 2/1 solution that was 1.8 mM in concentration. In separate 5 mL volumetric flasks, two different concentrations of lutidinium triflate solution (9.1 mmol/mL and 35.8 mmol/mL) were both prepared with the same solvent system. Subsequently, 0.2 mL of the 1.8 mM solution (0.00036 mmol) was transferred to a 1 cm path length quartz cuvette that was fitted with a rubber septum and diluted to 2~3 mL depending on how much acid solution needed to be added. An aliquot of the lutidinium triflate solution was taken up in a gastight syringe and sealed prior to removal from the drybox. The solution of acid was injected into the cuvette containing **1**. The reaction was immediately monitored after injection every 2, 3, 4, or 5 mins (details in figures) and temperature in the first 2.5 hours.

Variation of solvent system:

1 was weighted into a 2 mL volumetric flask and diluted to 2 mL to form a benzene solution that was 1.4 mM in concentration. Lutidinium triflate (3.1 mg) was weighted directly into a 1 cm path length quartz cuvette and 3 mL solution was prepared in the solvent of choice. A 0.2 mL aliquot of the **1** solution was taken up in a gastight syringe and sealed prior to removal from the drybox. Then, the solution of **1** was injected into the cuvette bringing the total volume to 3.2 mL. The reaction was immediately monitored after injection every 2, 4, or 5 mins in the first 2.5 hours at 26.4 °C.

UV-Vis spectra for the kinetic study

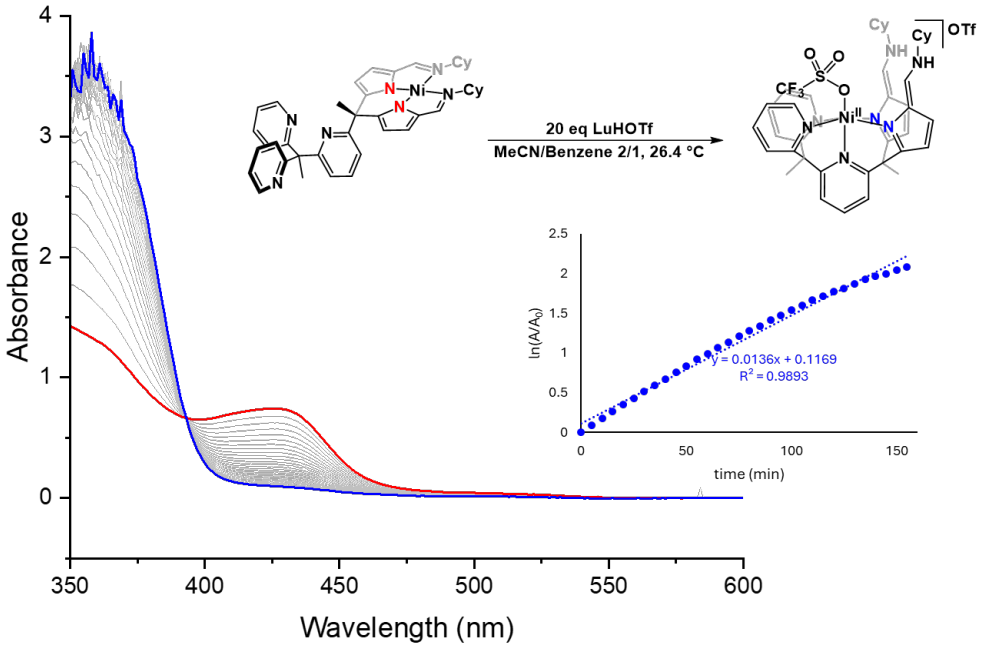

Figure S14. Time Resolved UV-visible Spectrum of 1 (0.11 mM) + 20 LuHOTf recorded every 5 min.

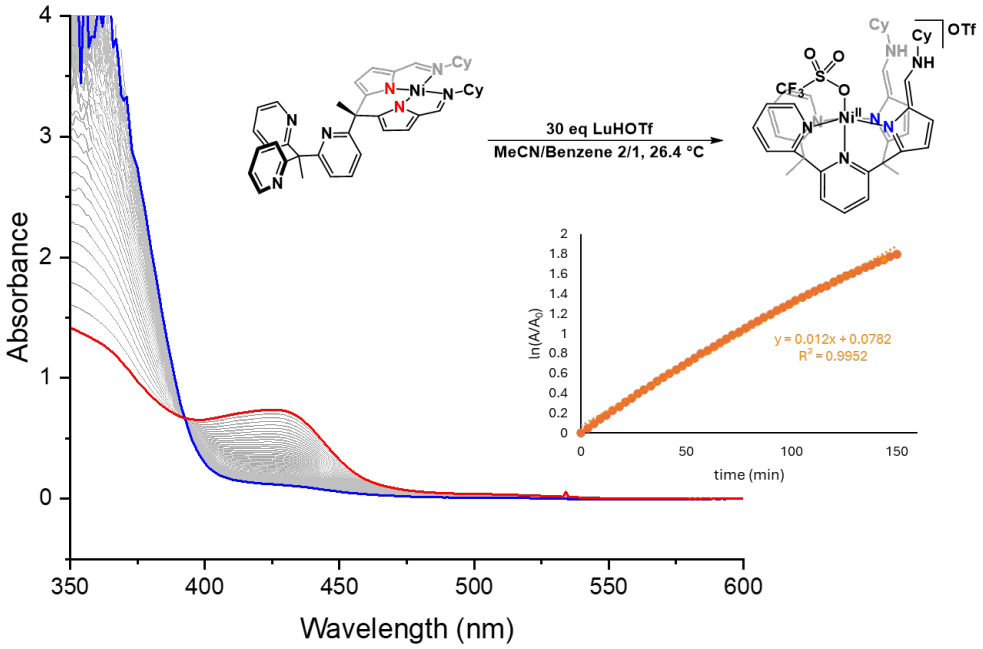

Figure S15. Time Resolved UV-visible Spectrum of 1 (0.10 mM) + 30 LuHOTf recorded every 3 min.

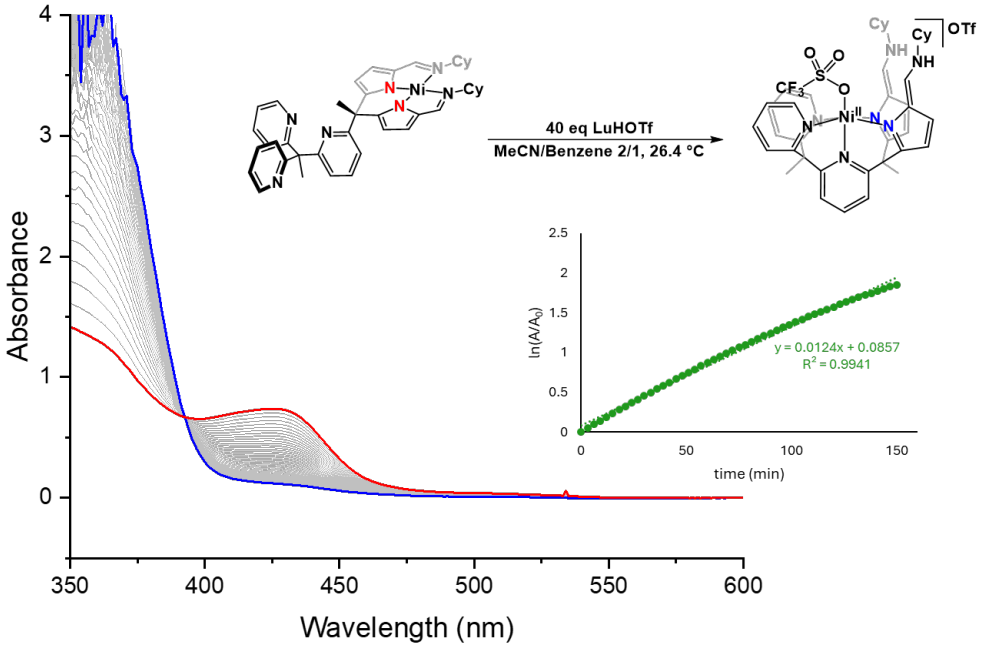

Figure S16. Time Resolved UV-visible Spectrum of 1 (0.10 mM) + 40 LuHOTf recorded every 3 min.

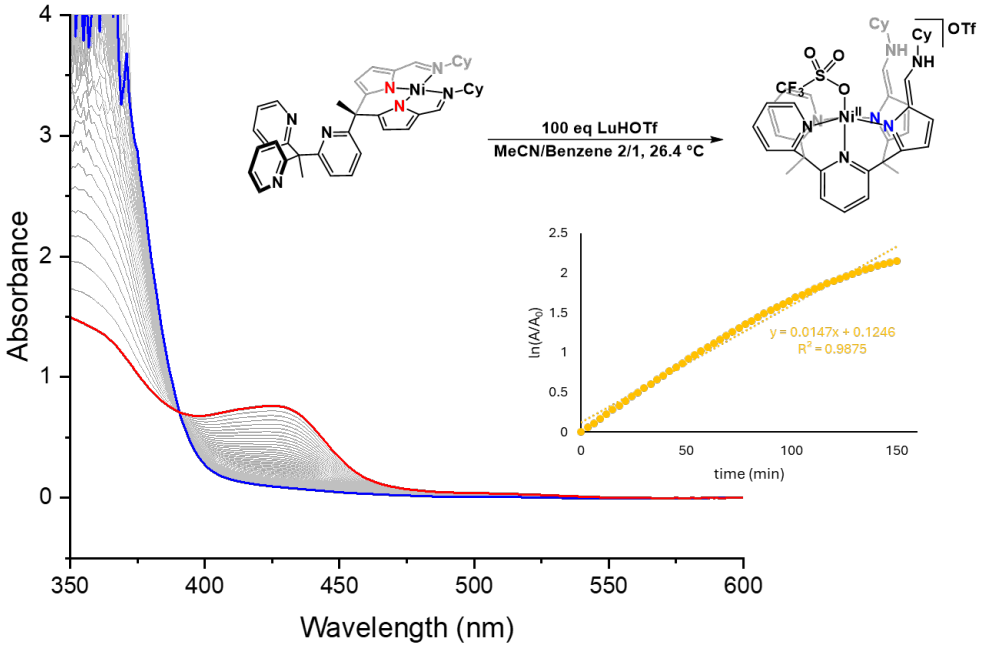

Figure S17. Time Resolved UV-visible Spectrum of **1** (0.10 mM) + 100 LuHOTf recorded every 3 min.

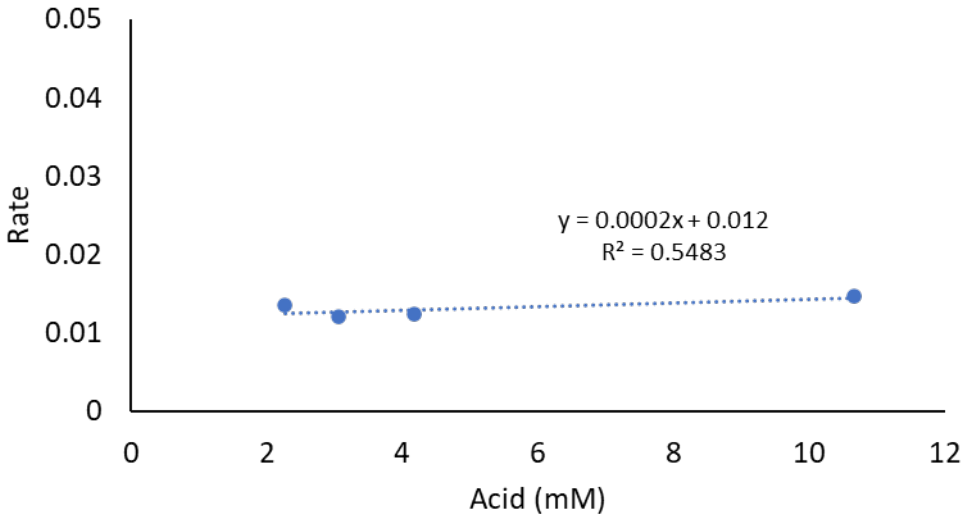

Figure S18. Reaction rate plot with various concentrations of acid.

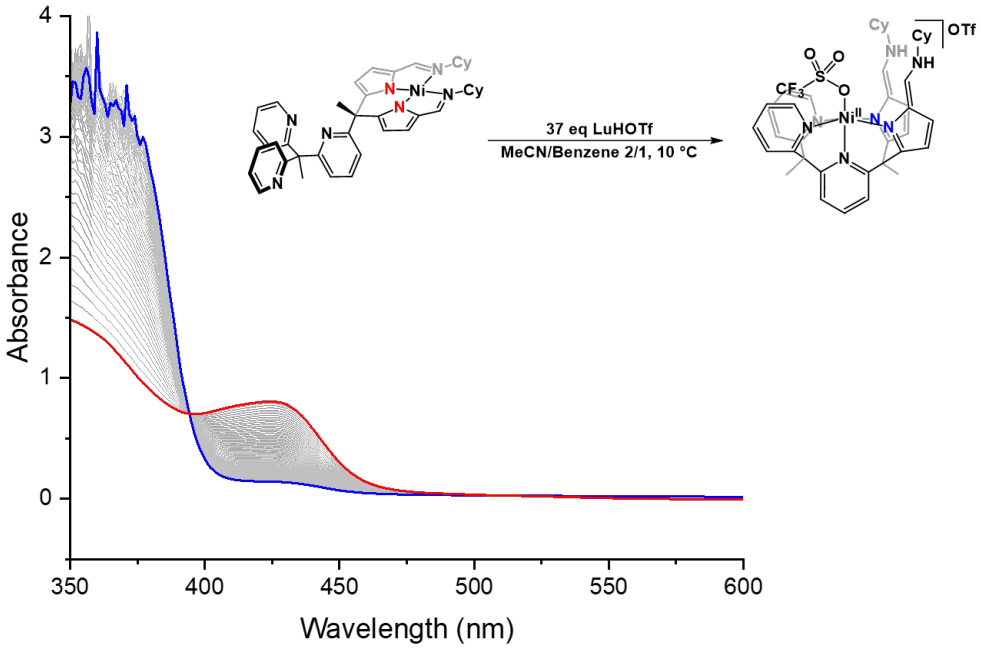

Figure S19. Time Resolved UV-visible Spectrum of **1** (0.12 mM) + 37 eq LuHOTf recorded every 5 min.

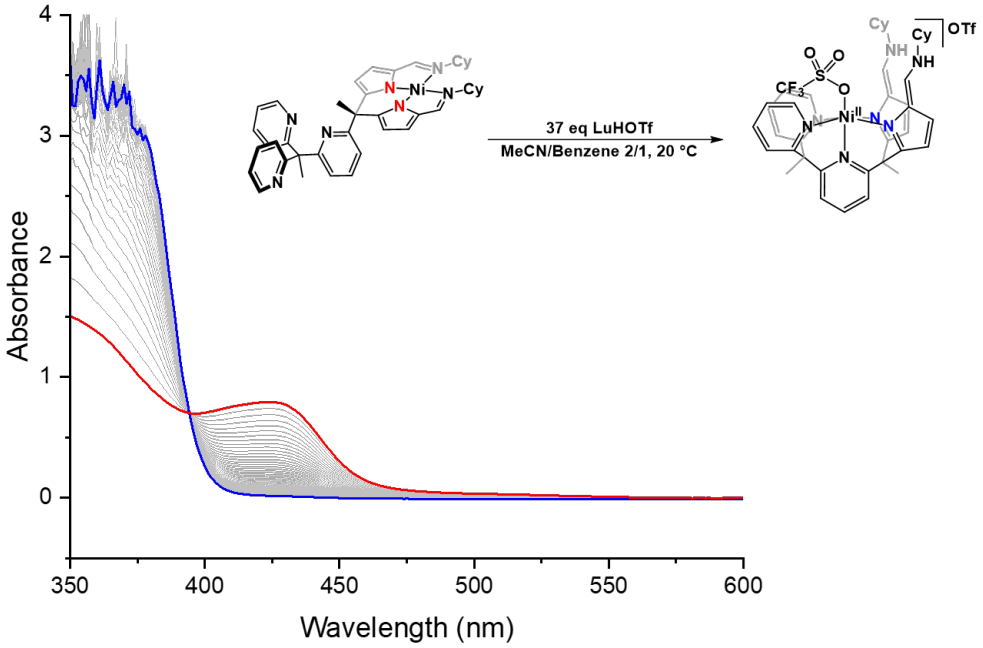

Figure S20. Time Resolved UV-visible Spectrum of **1** (0.12 mM) + 37 eq LuHOTf recorded every 5 min.

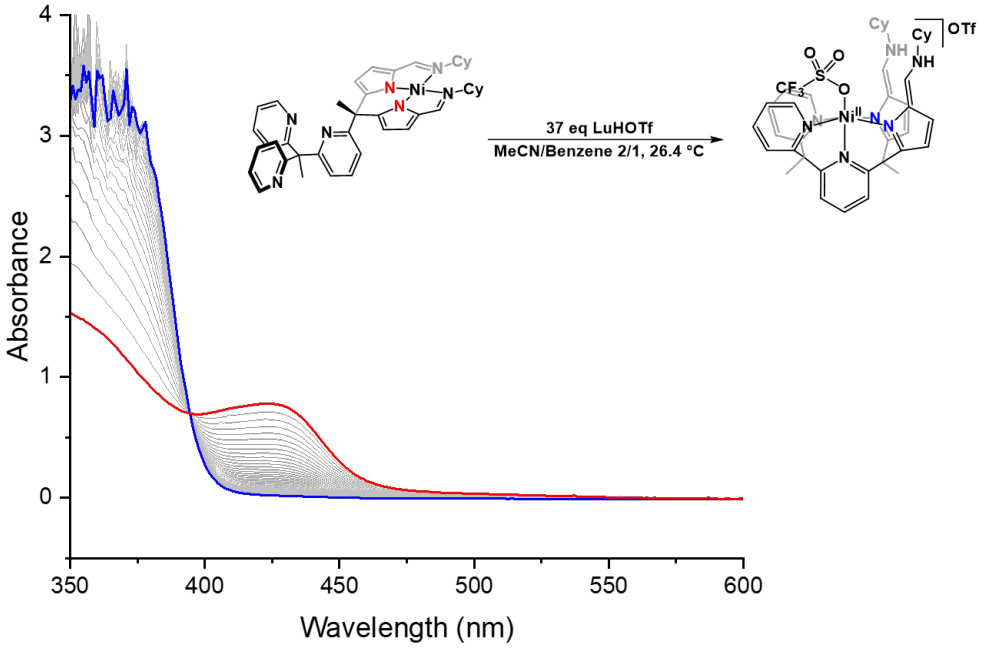

Figure S21. Time Resolved UV-visible Spectrum of **1** (0.12 mM) + 37 eq LuHOTf recorded every 4 min.

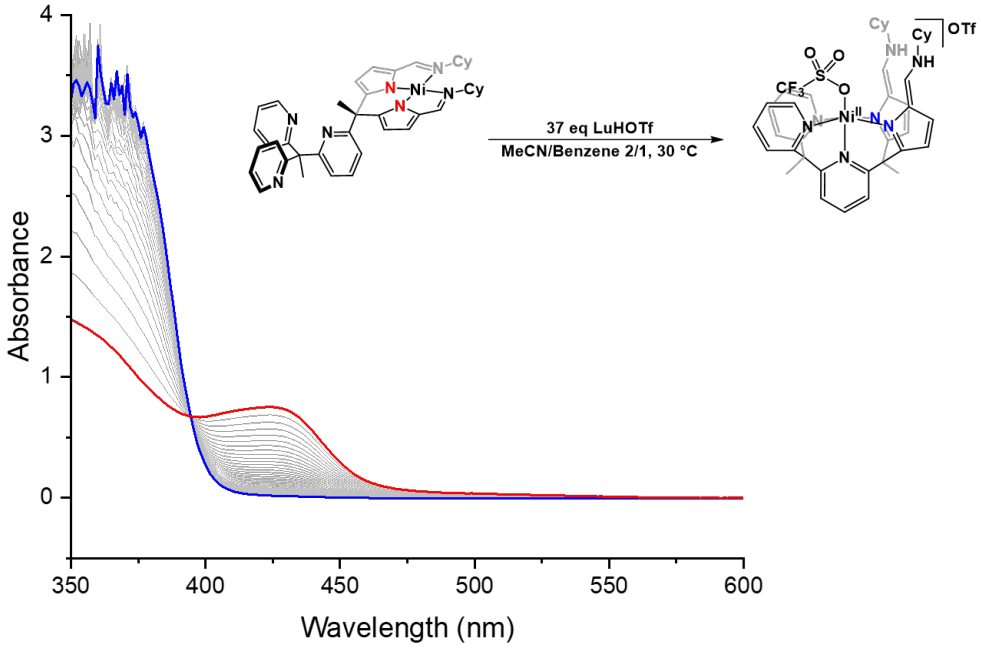

Figure S22. Time Resolved UV-visible Spectrum of **1** (0.12 mM) + 37 eq LuHOTf recorded every 3 min.

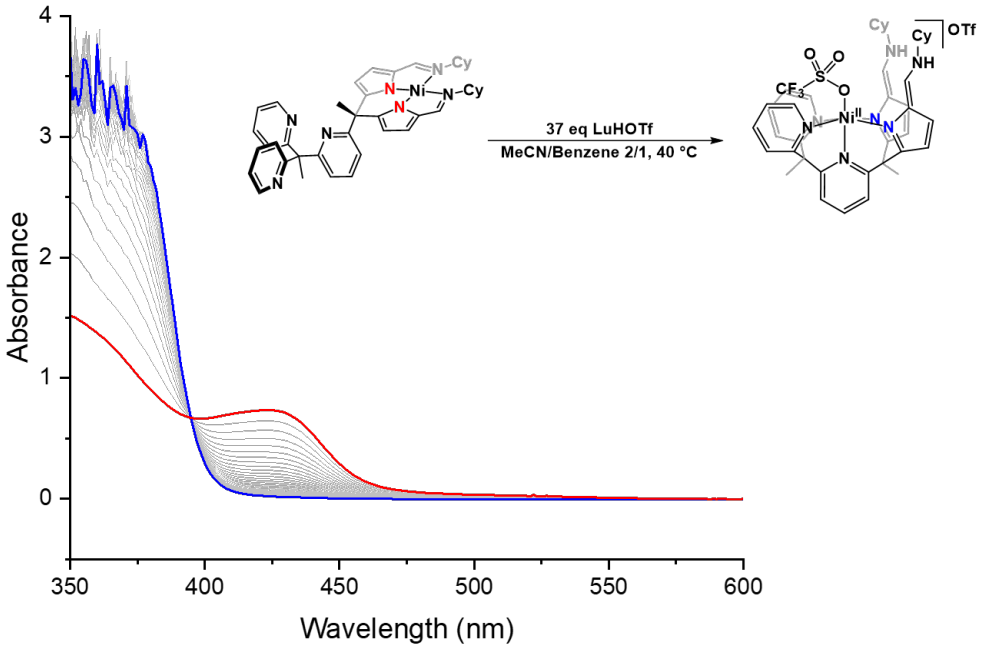

Figure S23. Time Resolved UV-visible Spectrum of **1** (0.12 mM) + 37 eq LuHOTf recorded every 2 min.

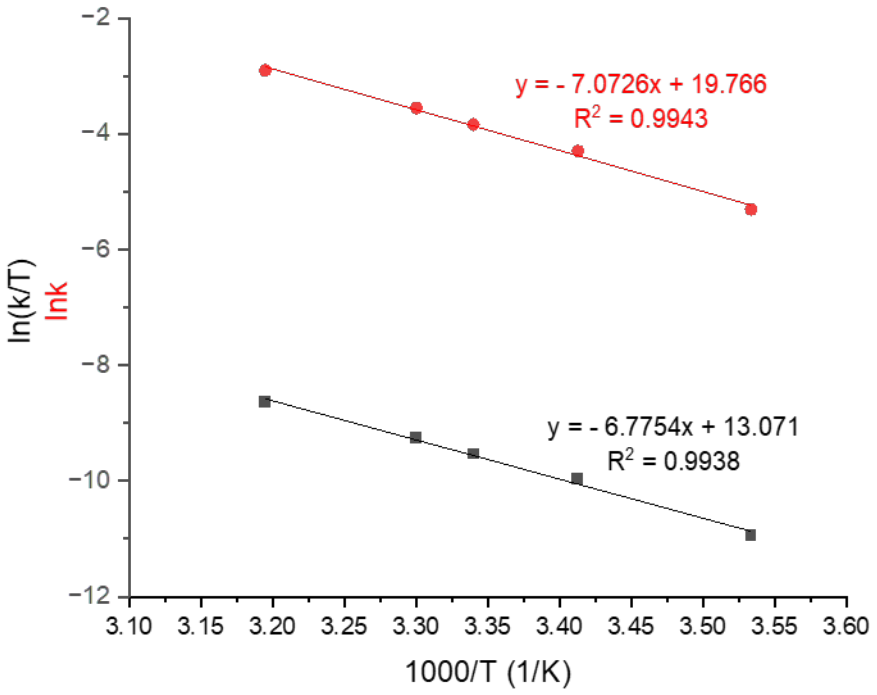

Figure S24. Eyring (black) and Arrhenius (red) plot

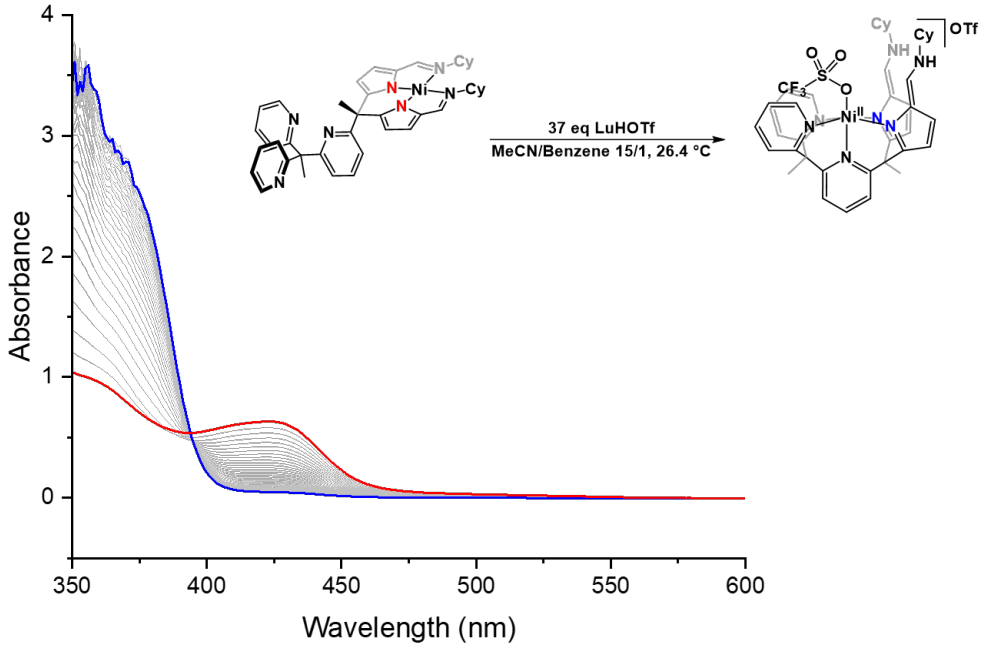

Figure S25. Time Resolved UV-visible Spectrum of **1** (0.09 mM) + 37 eq LuHOTf recorded every 2 min.

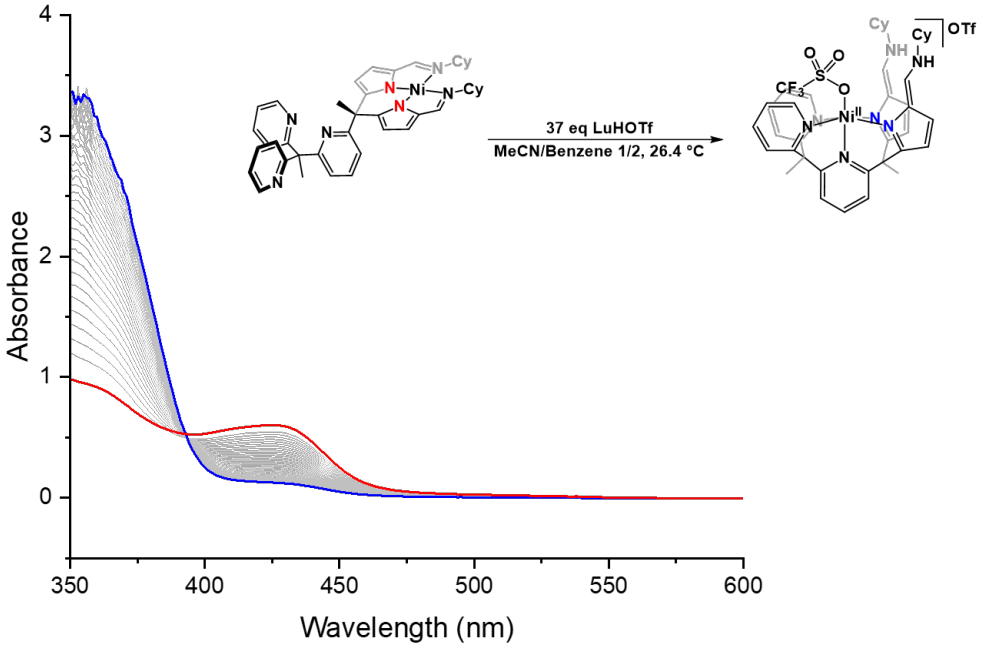

Figure S26. Time Resolved UV-visible Spectrum of 1 (0.09 mM) + 37 eq LuHOTf recorded every 4 min.

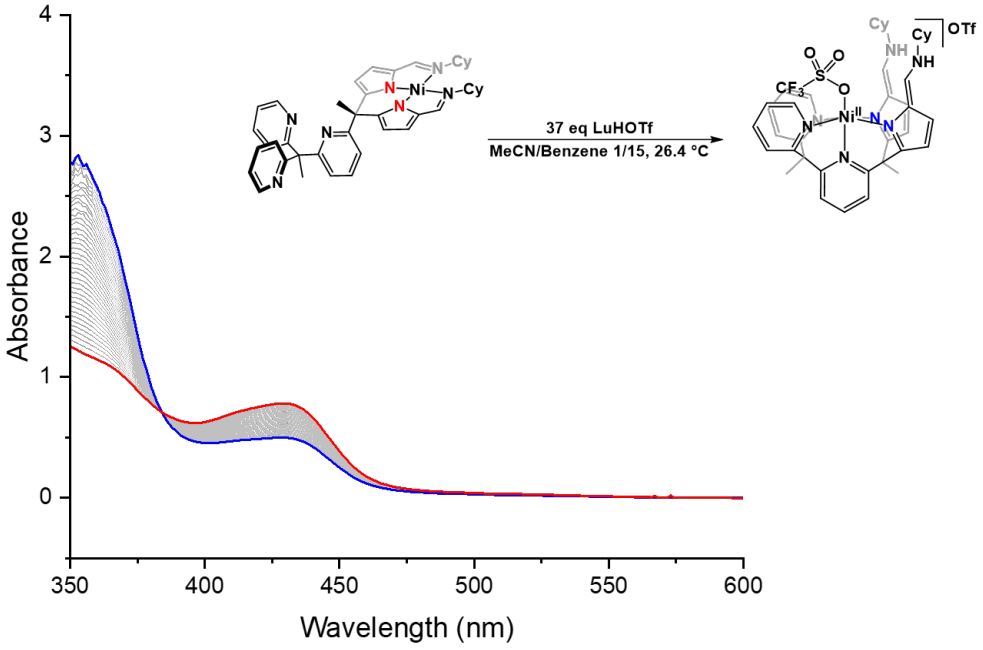

Figure S27. Time Resolved UV-visible Spectrum of **1** (0.09 mM) + 37 eq LuHOTf recorded every 4 min.

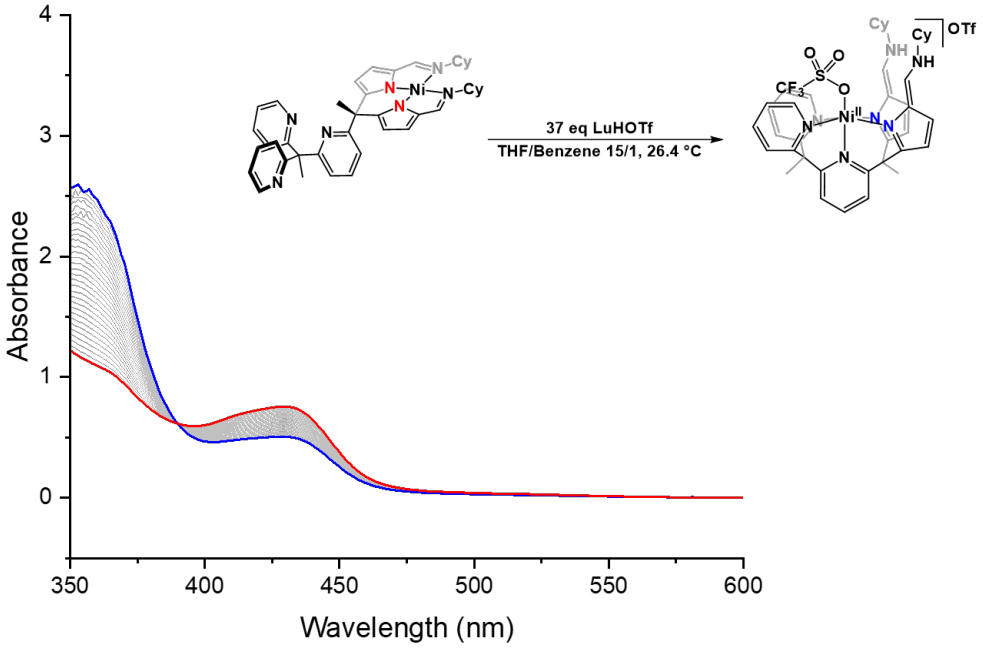

Figure S28. Time Resolved UV-visible Spectrum of **1** (0.09 mM) + 37 eq LuHOTf recorded every 5 min.

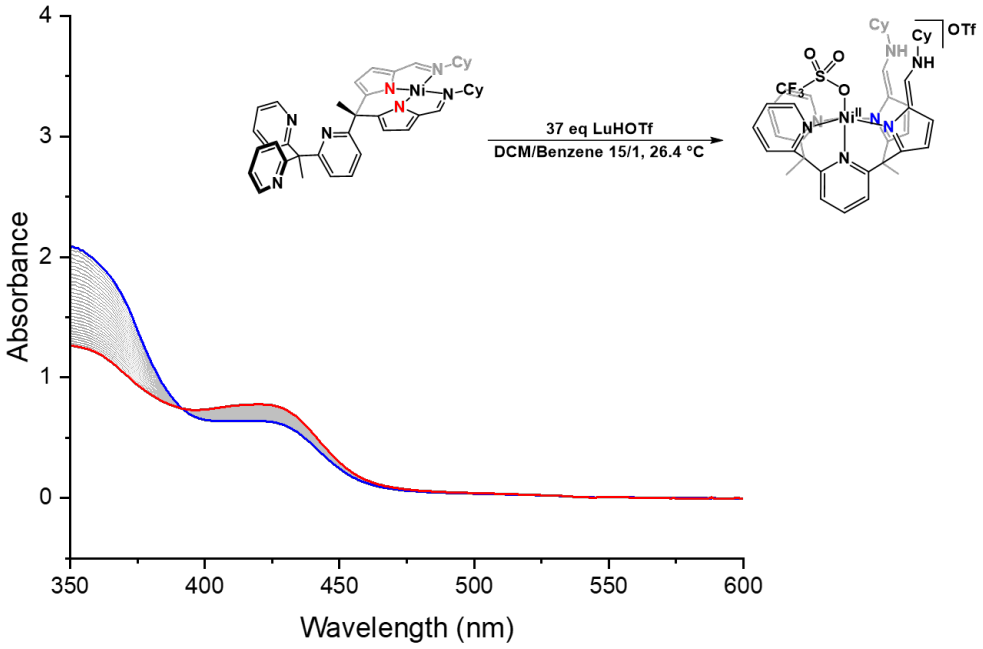

Figure S29. Time Resolved UV-visible Spectrum of **1** (0.09 mM) + 37 eq LuHOTf recorded every 5 min.

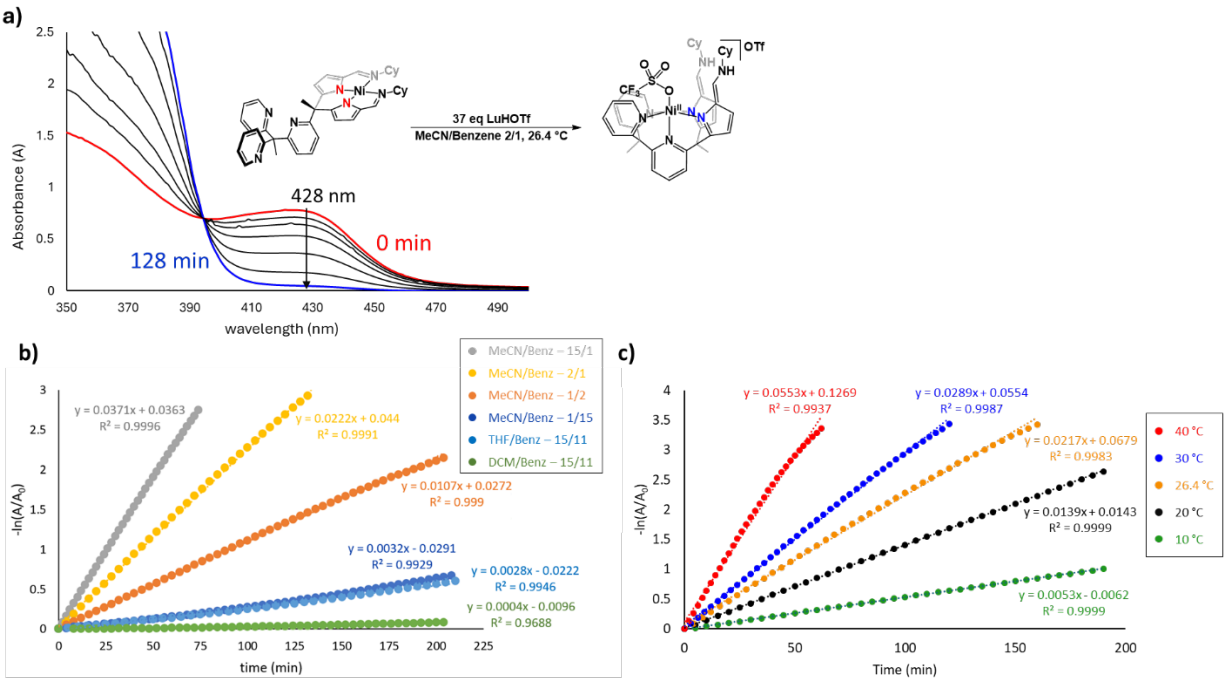

Figure S30. Summarized initial rates study of coordination change by **1** (0.12 mM) with excess of lutidinium triflate. a) Time Resolved UV-Vis spectrum. Rate plots of various b) solvent systems and c) temperatures.

Mechanistic study via NMR spectroscopy

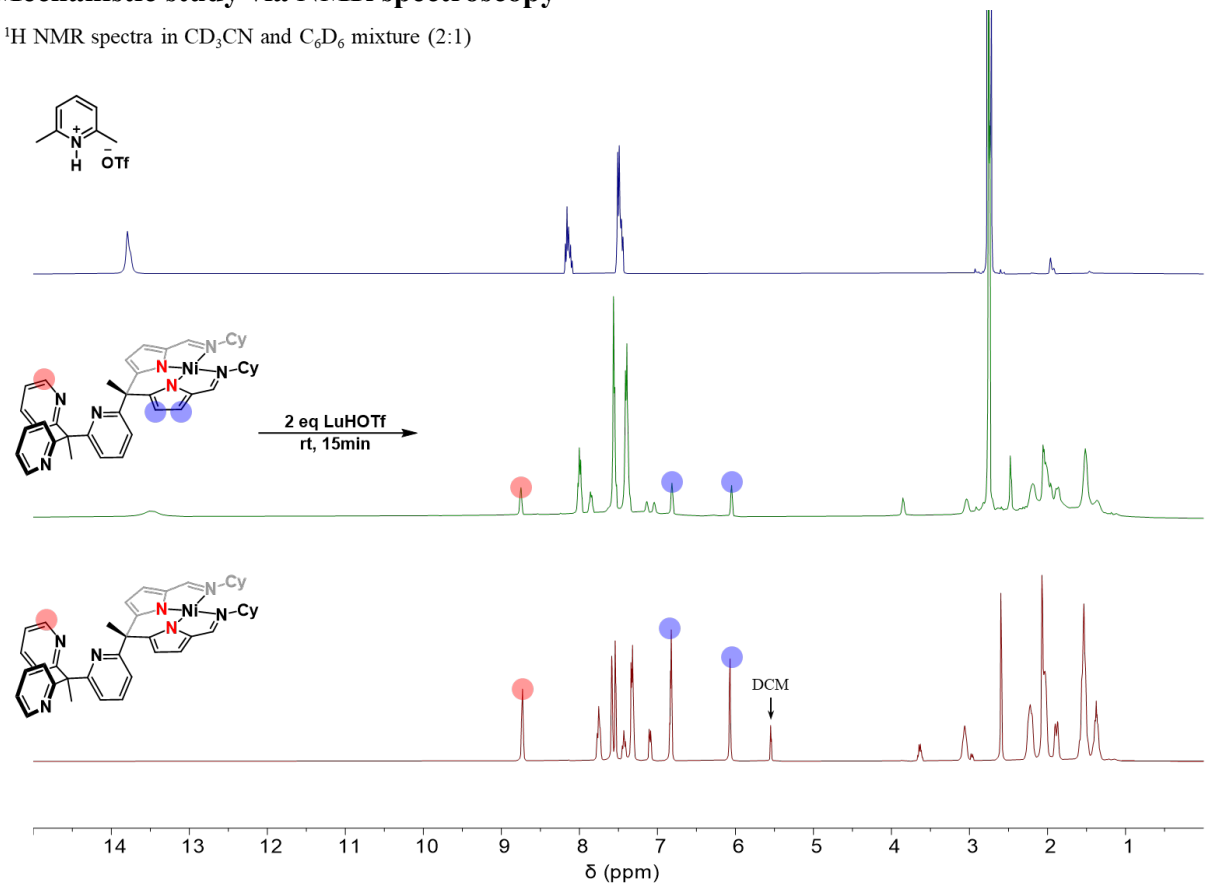

Figure S31. ^{1}H NMR of $Py_3(pi^{Cy})_2Ni$ + 2 eq lutidinium triflate after the first 15 min. (Slightly broad signal in the reaction was attributed to the paramagnetic $[Py_2Py(afa^{Cy})_2Ni]OTf_2$ started to form)

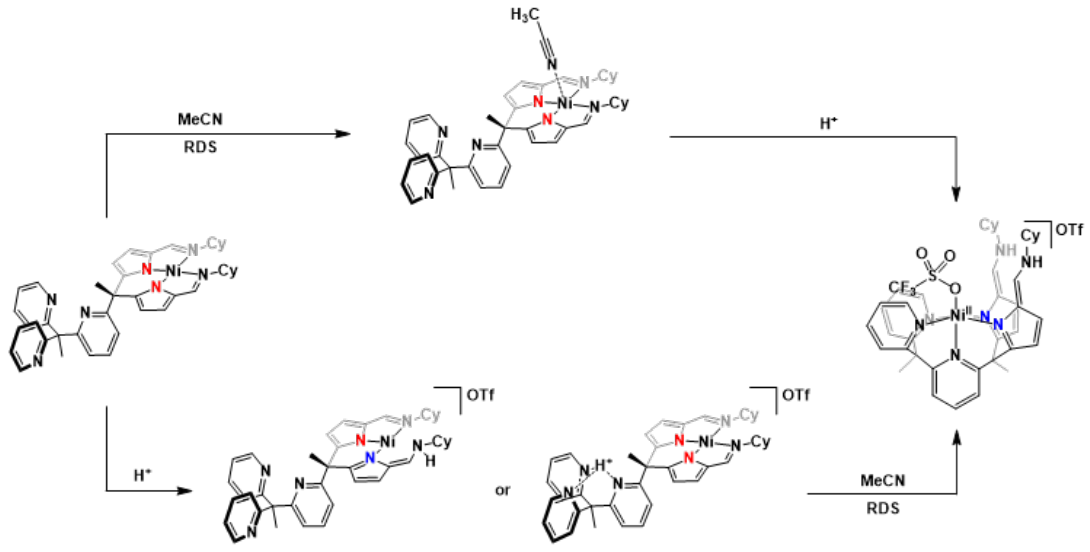

Scheme S1. Two possible mechanistic routes for geometrical change from **1** to **2**. (Top) acetonitrile coordination prior to protonation. (Bottom) Protonation followed by acetonitrile coordination.

Orbital interaction of $[Py_3(pi^{Cy})_2Ni(Ag)]OTf$

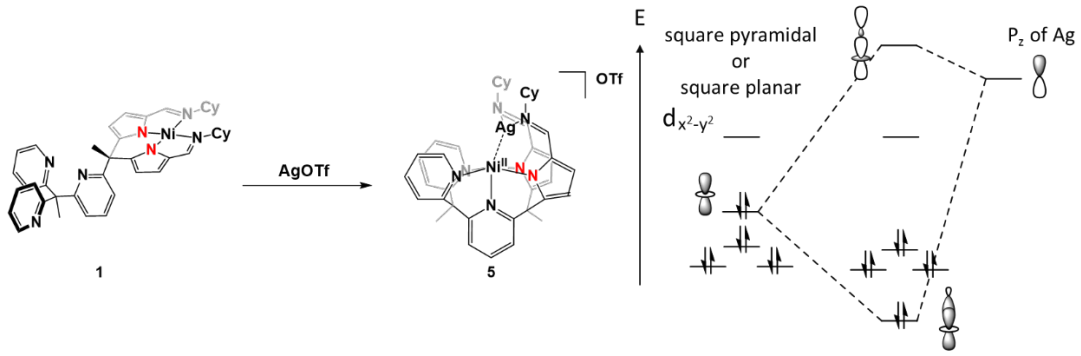

Figure S32. Proposed orbital interaction diagram for a coordinated square planar or square pyramidal nickel(II) complex and a Z-type silver ligand

Solid-state structures

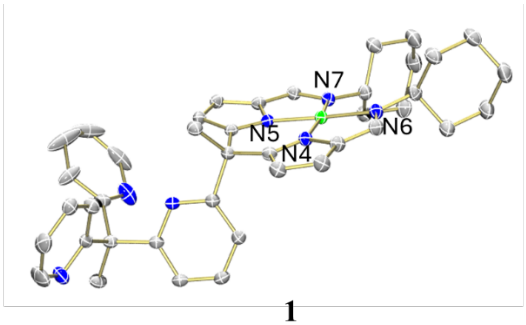

1

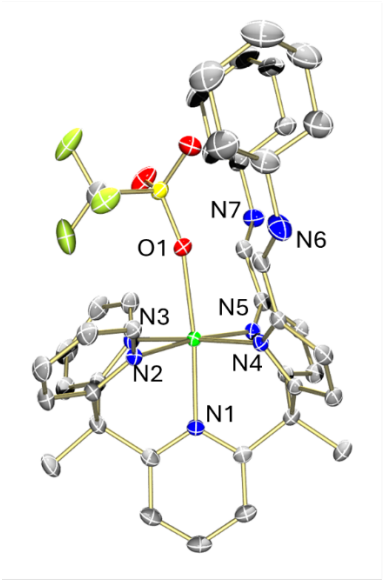

2

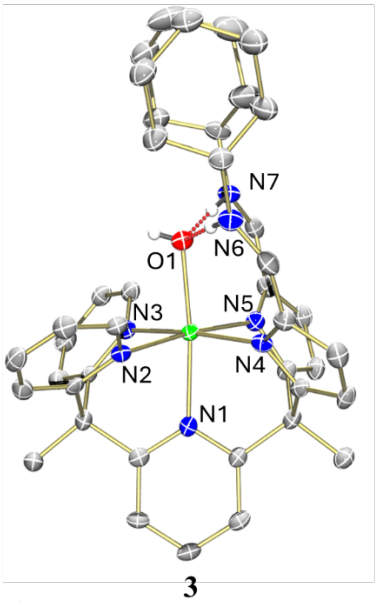

3

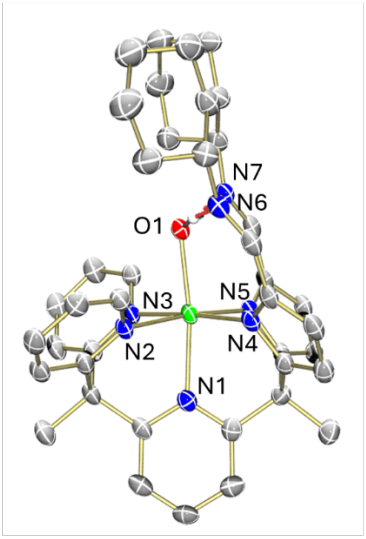

4

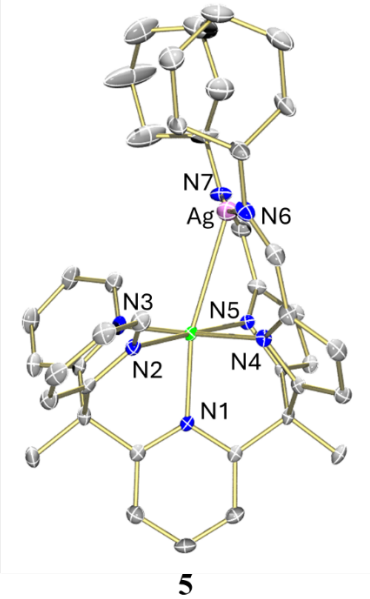

5

Figure S33. Molecular structures of **1** to **5** with 50% probability ellipsoids. Solvents, outer sphere ions, and selected hydrogen atoms are omitted for clarity.

Crystallographic Parameters

Table S1. Selected bond lengths and angles for 1-5.

	1	**2**	**3**	**4**	**5**
Ni-$N_{pi(avg)}$	1.8409(2)			2.1025(4)	2.0545(3)
N-$N_{afa(avg)}$		2.0868(14)	2.1045(4)		
Ni-$N_{py(avg)}$		2.1004(15)	2.129(4)	2.227(4)	2.0905(3)
Ni-N_1		2.1053(15)	2.109(4)	2.112(4)	2.041(3)
Ni-O_1		2.2011(13)	2.045(4)	2.069(3)	
$N_{6/7(avg)}$--(H)--O_1			2.638(6)	2.730(5)	
Fe–O_1–$N_{6/7(avg)}$			102.21(17)	102.48(13)	

Table S2. Crystal data and structure refinement for **1**, **2**, and **3-PF_6**.

	$Py_3(pi^{Cy})_2Ni$ **1**	$[Py_2Py(afa^{Cy})_2Ni]OTf_2$ **2**	$[Py_2Py(afa^{Cy})_2Ni(OH)]PF_6$ **3-PF_6**
Empirical Formula	C84 H96 Cl4 N14 Ni2	C45 H50 F6 N8 Ni O6 S2	C43 H52 Cl4 F6 N7 Ni O P
Formula Weight	1558.95	1035.76	1028.40
Temperature	100.00 K	100.00 K	110.00 K
Radiation	CuKα (λ = 1.54184 Å)	CuKα (λ = 1.54184 Å)	MoKα (λ = 0.71073 Å)
Crystal system	Monoclinic	Orthorhombic	Monoclinic
Space group	$P2_1/c$	P*bca*	$C2_1/c$
Unit Cell Parameters	a = 38.7270(2) Å b = 8.71219(5) Å c = 22.27255(11) Å α = 90.00° β = 94.0610(5)° γ = 90.00°	a = 18.22020(10) Å b = 21.21480(10) Å c = 24.43120(10) Å α = 90.00° β = 90.00° γ = 90.00°	a = 24.699(3) Å b = 14.4845(16) Å c = 25.529(3) Å α = 90.00° β = 93.835(3) ° γ = 90.00°
Volume	7495.83(7)	9443.59(8)	9112.6(17)
Z	4	8	8
Reflections collected	141776	91427	48042
Independent reflections	15972	10166	7928
Goodness-of-fit on F^2	1.032	1.029	1.058
Final R indexes [I>=2σ(I)]	R_1 = 0.0610 wR_2 = 0.1649	R_1 = 0.0431 wR_2 = 0.1125	R_1 = 0.0706 wR_2 = 0.1827

Table S1. Crystal data and structure refinement for **4**, and **5**.

	$Py_2Py(pi^{Cy})_2NiOH_2$ **4**	$[Py_2Py(afa^{Cy})_2Ni]OTf_2$ **5**
Empirical Formula	C44 H53 Cl6 N7 Ni O	C42 H45 Ag F3 N7 Ni O3 S
Formula Weight	967.34	951.49
Temperature	110.0 K	110.0 K
Radiation	CuKα (λ = 1.54178 Å)	CuKα (λ = 1.54178 Å)
Crystal system	Triclinic	Monoclinic
Space group	P-1	$P2_1/n$
Unit Cell Parameters	a = 12.6855(4) Å b = 13.1657(4) Å c = 13.8011(5) Å α = 90.462(2)° β = 93.570(2)° γ = 100.570(2)°	a = 10.8971(10) Å b = 15.1770(14) Å c = 24.243(2) Å α = 90.00° β = 102.067(3)° γ = 90.00°
Volume	2259.67(13)	3920.9(6)
Z	2	4
Reflections collected	58726	54684
Independent reflections	8018	7470
Goodness-of-fit on F^2	1.057	1.066
Final R indexes [I>=2σ(I)]	R_1 = 0.0691 wR_2 = 0.1810	R_1 = 0.0451 wR_2 = 0.1327

References:

1. Curley, J.J., Bergman, R.G., and Tilley, T.D., *Dalton Trans.*, **2012**. *41*, 192-200.
2. Drummond, M.J., Ford, C.L., Gray, D.L., Popescu, C.V., and Fout, A.R., *J. Am. Chem. Soc.*, **2019**. *141*, 6639-6650.
3. APEX3 (V2019.1-0). Bruker AXS Inc.: Madison, WI 2019.
4. Sheldrick, G. M. SADABS. University of Grottingen, Germany 2016.
5. Sheldrick, G., *Acta Crystallogr.*, **2015**. *A-71*, 3-8.
6. Sheldrick, G.M., *Acta Crystallogr.*, **2015**. *C-71*, 3-8.
7. Dolomanov, O.V., Bourhis, L.J., Gildea, R.J., Howard, J.A.K., and Puschmann, H., *J. Appl. Crystallogr.*, **2009**. *42*, 339-341.
8. Diffraction, R. O. CrysAlisPro Software System,. Rigaku Oxford Diffraction 2023.